JQ-1 ameliorates schistosomiasis liver fibrosis by suppressing JAK2 and STAT3 activation

Short title: JQ-1 ameliorates schistosomiasis liver fibrosis through JAK2/STAT3

Han Ding[1¶], Jiaming Tian[1¶], Xuhan Yang[1], Yongsheng Ji[1], Saeed El-Ashram[2], Xin Hou[1], Cuiping Ren[1], Jijia Shen[1]*, Miao Liu[1]*

1. Department of Microbiology and Parasitology, Anhui Provincial Laboratory of Microbiology and Parasitology, Anhui Key Laboratory of Zoonoses, School of Basic Medical Sciences, Anhui Medical University, 81#Meishan Road, Hefei, Anhui 230032, People's Republic of China ; 2.College of Life Science and Engineering, Foshan University, 18 Jiangwan Street, Foshan, Guangdong 528231 People's Republic of China

¶These authors contributed equally to this work.

*Corresponding author:

Miao Liu, E--mail: iammiaoliu@126.com

Jijia Shen, E--mail:shenjijia@hotmail.com

Abstract

Schistosomiasis is a serious parasitic infection caused by *Schistosoma*. The parasite deposits eggs in the host liver, causing inflammation that activates hepatic stellate cells (HSCs), which leads to liver fibrosis. Currently, there is no effective therapy for liver fibrosis; thus, treatments are urgently needed. Therefore, in the present study, mice infected with *Schistosoma japonicum* were treated with JQ-1, a small-molecule bromodomain inhibitor with reliable anti-tumor and anti-inflammatory activities. The fibrotic area of the liver measured by computer-assisted morphometric analysis and the expression levels of the cytoskeletal protein alpha smooth muscle actin (α-SMA) and of collagen assessed by quantitative PCR and immunohistochemistry were significantly decreased in the liver following JQ-1 treatment compared with vehicle-treated controls. Total RNA was extracted from the liver of JQ-1–treated *Schistosoma*-infected mice for RNA-sequencing analysis. Gene ontology and Kyoto Encyclopedia of Genes and Genomes analyses indicated that JQ-1 affected biological processes and the expression of cellular components known to play key roles in HSC transdifferentiation into myofibroblasts. In vitro treatment with JQ-1 of JS-1 cells, a mouse HSC line, indicated that JQ-1 significantly inhibited JS-1 proliferation but had no effect on JS-1 activity, senescence, or apoptosis. Western blot results showed that JQ-1 inhibited the expression of phosphorylated JAK2 and phosphorylated STAT3 without altering expression levels of these non-phosphorylated proteins. Taken together, these findings suggested that JQ-1 treatment ameliorated *S. japonicum* egg–induced liver fibrosis, at least in part, by suppressing HSC activation and proliferation through the inhibition of JAK2/STAT3 signaling. These results lay a foundation for the development of novel approaches to treat and control liver fibrosis caused by *S. japonicum*.

Key words: Schistosoma japonicum; Fibrosis; JQ-1; JAK2/STAT3

Author summary

When a host is infected with *Schistosoma,* a common parasite that affects more than a million people and hundreds of thousands of livestock, the parasite deposits eggs in the liver of the host. The eggs lead to liver inflammation, which activates stellate cells in the liver. These stellate cells generate most of the excessive extracellular matrix that replaces healthy liver parenchyma with fibrous tissue, causing liver fibrosis. *Schistosoma japonicum* causes the most severe liver damage of all the schistosome parasites. Therefore, inhibiting the activation of the liver stellate cells and removing the activated stellate cells are key strategies for treating liver fibrosis caused by this parasite. JQ-1 is a potent inhibitor of the BET family of bromodomain proteins and is structurally similar to inhibitors being tested in clinical trials for various types of cancers. Here we found that administering JQ-1 to mice infected with *S. japonicum* decreased the degree of liver fibrosis. JQ-1 inhibited the activation and proliferation of liver stellate cells by blocking the phosphorylation and thus the activation of JAK2 and STAT3 to achieve its therapeutic effects. Thus, this study provides insights into the development of new therapeutic strategies for *Schistosoma*-induced liver fibrosis.

Key words: *Schistosoma japonicum*; Fibrosis; JQ-1; JAK2/STAT3

1. Introduction

Among the three major schistosomes known to infect humans (*Schistosoma japonicum*, *Schistosoma mansoni*, and *Schistosoma haematobium*), *S. japonicum* causes the most severe pathological damage. In China, *S. japonicum* is a common parasite associated with chronic liver fibrosis [1]. Currently, zoonotic schistosomiasis caused by *S. japonicum* is major public health threat affecting more than a million people and hundreds of thousands of livestock in China [1]. Egg-induced lesions in the liver and intestinal wall of the host are important complications of infection with *S. japonicum*. The immune response of the host to the eggs results in granuloma and fibrosis [2]. Because the mechanism of fibrosis is not fully understood, there is no effective therapy for liver fibrosis. Although the U.S. Food and Drug Administration (FDA) has recently approved pirfenidone and nintedanib as treatments, additional new therapies are needed for treating liver fibrosis [3].

The bromodomain and extra-terminal (BET) family contains four members (bromodomain motif-containing proteins BRD2, BRD3, BRD4, and BRDT) that specifically recognize acetylated lysine residue sites and participate in the regulation of epigenetic protein expression, which plays a key role in regulating various biological processes, including inflammation, the cell cycle, maintenance of the higher-order chromatin structure, and identification of DNA damage signals [4-5]. JQ-1 is a selective inhibitor of the BET family and has been shown to have promising anti-tumor and anti-inflammation effects [6]. JQ-1 has been found to inhibit the development of fibrosis in both a mouse model of hepatic fibrosis induced by carbon tetrachloride (CCl4) and a mouse model of bleomycin-induced pulmonary fibrosis [7-8]. Therefore, we hypothesized that JQ-1 would be effective in the treatment of hepatic fibrosis caused by *S. japonicum*. However, little is known about the mechanisms underlying the effect

of JQ-1 on hepatic fibrosis caused by *S. japonicum*.

Therefore, the aim of the present study was to explore the mechanisms of action underpinning the therapeutic effect of JQ-1 by using a mouse model of hepatic fibrosis naturally caused by *S. japonicum*. We found that the degree of liver fibrosis in mice treated with JQ-1 was significantly decreased, mainly through inhibiting the activation and proliferation of hepatic stellate cells (HSCs). The activation and proliferation of HSCs were inhibited by decreasing the phosphorylation and thus activation of Janus kinase 2 (JAK2) and signal transducer and activator of transcription 3 (STAT3). These findings lay a foundation for the development of new approaches for the treatment and control of liver fibrosis caused by *S. japonicum*.

2. Materials and methods

2.1. Ethics statement

All animal experiments were approved by the Institutional Animal Care and Use Committee at Anhui Medical University (Approval Number: LLSC20140061) and conformed to the guidelines outlined in the Guide for the Care and Use of Laboratory Animals. All infection was performed under anesthesia, and all efforts were made to minimize suffering.

2.2. Mouse model of fibrosis, cell culture, and reagents

Female C57BL/6 mice (6 weeks old) were purchased from the Experimental Animal Center of Anhui Province in Hefei, China. Mice were housed under specific pathogen-free conditions at Anhui Medical University, with free access to food and water food. The protocols for the animal experiments were approved by the Institutional Animal Care and Use Committee at Anhui Medical University. Freshwater

118 *Oncomelania hupensis* snails infected with *S. japonicum* (provided by Hunan
119 Provincial Institute of Parasitic Diseases in China) were exposed to light for 3–4 h (25–
120 28 °C) to induce the release of cercariae. Hepatic fibrosis was experimentally induced
121 in 18 mice by infecting them with 18 ± 2 of these cercariae through the skin of abdomen.
122 The infected mice were randomly divided into two groups, experimental and control,
123 with nine mice in each group.
124
125 Six weeks after the infection, the mice were treated with praziquantel by intragastric
126 gavage (500 mg/kg/d for 2 days). In the seventh week, mice in the experimental group
127 were injected intraperitoneally (I.P.) with JQ-1 (50 mg/kg body weight/day; Cat. No.
128 HY-13030, MedChem Express; USA), and mice in the control group were injected I.P.
129 with vehicle, that is, (2-hydroxypropyl)-β-cyclodextrin (HP-β-CD; Cat. No. 778966,
130 Sigma; USA) 10% (wt/vol), once daily for 15 days. Animals were humanely killed 24
131 h after the final injection. They serum and the liver from each mouse were collected for
132 subsequent experimental analyses.
133
134 The murine HSC line, JS-1 cells, had been previously purchased from BeNa Culture
135 Collection (Beijing, China) and preserved in our laboratory. For the present study, JS-
136 1 cells were cultured in Dulbecco's modified Eagle medium with 10% fetal bovine
137 serum.
138
139 **2.3. Egg count in liver tissue**
140 Potassium hydroxide (10%; 1 mL) was added to 0.1 g of liver tissue and digested at 37
141 °C for 2 h. The number of eggs in the sample was then counted using a light microscope.
142

2.4. Assessment of liver fibrosis

Sections (5 μm thick) of formalin-fixed, paraffin-embedded liver specimens were stained with Sirius red. The red-stained collagen fibers were quantified by determining the percentage of the stained area per total liver section as measured by computer-assisted morphometric analysis. Immunostaining for alpha smooth muscle actin (α-SMA), a marker for a subset of activated fibrogenic cells and myofibroblasts, and collagen Ia1 (Col1a1) was performed using polyclonal α-SMA at a dilution of 1:500 and Col1a1 (1:250) primary antibodies (Bioss Inc.; Beijing, China). Immunohistochemical analysis was performed with the PowerVision two-step detection system (Zhongshan Biotechnology Co.; Beijing, China). Six to ten photomicrographs per mouse liver were captured using an inverted microscope (Nikon 80I, Japan). Quantitative and qualitative changes were analyzed using morphometric software (Image-Pro Plus; Media Cybernetics). At least three noncontinuous tissue sections were measured, and the mean values obtained from nine mice were used for statistical analysis.

Hydroxyproline content has been described as a surrogate for collagen content in fibrogenesis. We measured the hydroxyproline content of the liver using a commercial kit (Nanjing Jiancheng Bioengineering Institute; China). Briefly, 1 mL of hydrolysate was added to a liver tissue sample (0.1 g), mixed, and fermented/heated in a boiling water bath for 20 min. The suspension was mixed every few minutes to hydrolyze the tissue components. The resulting components were used to detect the hydroxyproline content according to the kit manufacturer's instructions. Absorbance was read at a wavelength of 550 nm, and the total hydroxyproline content in the samples was extrapolated from a standard curve.

168

169 **2.5. Serum liver enzyme quantification**

170 The levels of serum alanine aminotransferase (ALT) and aspartate aminotransferase
171 (AST) were determined using a serum aminotransferase test kit (Nanjing Jiancheng
172 Bioengineering Institute; China) according to the manufacturer's instructions and
173 reported in terms of units per liter.

174

175 **2.6. RNA sequencing and data analysis**

176 Three individual liver samples from each group were pooled to generate one sample for
177 RNA sequencing. Liver samples were finely ground, and total RNA was extracted using
178 TRIzol (Invitrogen; Carlsbad, CA, USA). The quantity and purity of the total RNA
179 were assessed using a Bioanalyzer 2100 system. A 5-μg sample of total RNA was used
180 to isolate poly(A) mRNA with a poly(T) oligo primer attached to magnetic beads
181 (Invitrogen). Briefly, mRNA was extracted from total RNA using oligo (dT) magnetic
182 beads and sheared into short fragments. These fragments of mRNA were then used as
183 templates for cDNA synthesis. The cDNAs were amplified by polymerase chain
184 reaction (PCR) to complete the library. The cDNA library was constructed from the
185 RNA samples and sequenced with an Illumina Hiseq 2500 system according to the
186 manufacturer's instructions. Differentially expressed genes were submitted to
187 enrichment analysis by gene ontology (GO) and Kyoto Encyclopedia of Genes and
188 Genomes (KEGG). *P* values were calculated using the Benjamini-corrected modified
189 Fisher's exact test, and $P \leq 0.05$ was considered statistically significant.

190

191 **2.7. Quantitative PCR**

Total RNA was extracted from the liver of each mouse. The mRNA was reverse transcribed to cDNA using a PrimeScript RT reagent kit (Takara; Dalian, China). Real-time reverse transcription quantitative PCR (qPCR) was performed in duplicate using 1 μL of cDNA from each sample and SYBR Premix Ex Taq Ⅱ (Takara) according to the manufacturer's instructions. All reactions were performed using an ABI-Prism StepOnePlus sequence detector system under the following conditions: 10 s at 95 °C; 40 cycles of 15 s at 95 °C and 40 s at 60 °C followed by 15 s at 95 °C; 1 min at 60 °C; and 95 °C for 15 s. This allowed for the generation of a standard regression curve using threshold settings and software analysis. Primers for qPCR were designed and synthesized by Sangon Biotech Co. Ltd. Quantification was performed by comparing the cycle threshold (Ct) values of each sample after normalization to GAPDH. Primer sequences are summarized in Supplementary Table 1. The relative quantification levels were calculated using the $2^{(-\Delta\Delta CT)}$ method.

2.8. Cell viability assay

The mouse HSC line JS-1 cells were cultured on six-well chamber slides in the presence of DMSO (0.1%) or JQ-1 (500 nM) for 24 h. The exponentially growing cells were trypsinized and washed twice with phosphate-buffered saline (PBS). Then, 450 μL of cell suspension was mixed with 50 μL of 0.4% trypan blue dye and left for 5 min at room temperature. Trypan blue exclusion was assessed, viable cells were counted using a hemocytometer, and the percentage of viable cells was determined.

2.9. Cell proliferation assay

JS-1 cells were cultured on six-well chamber slides in the presence of DMSO (0.1%) or JQ-1 (500 nM) for 24 h. The Cell Counting Kit-8 (CCK-8; Dojindo Laboratories;

Japan) solution (10 μL/well) was added to measure cell proliferation at specific intervals (0, 12, and 24 h of incubation). After 2 h of further incubation at 37 °C in 5% CO_2, the absorbance of each well was measured at a wavelength of 450 nm by a Model 680 microplate reader (Bio-Rad; Richmond, CA, USA).

2.10. Terminal deoxynucleotidyl transferase dUTP nick end labeling (TUNEL) Assay

JS-1 cells were cultured on six-well chamber slides in the presence of DMSO (0.1%) or JQ-1 (500 nM) for 24 h. After incubation, JQ-1–induced apoptosis of JS-1 cells was determined using a One-Step TUNEL Apoptosis Assay Kit (Beyotime; China) according to the manufacturer's instructions. Briefly, JQ-1–treated cells were washed twice with ice-cold PBS, fixed with 4% paraformaldehyde for 30 min, and permeabilized with 0.5% Triton X-100 for 5 min. The cells were subsequently incubated with the TUNEL detection reagent at 37 °C for 1 h. Cell fluorescence was observed under a fluorescence microscope.

2.11. Senescent cell staining

JS-1 cells cultured on six-well chamber slides in the presence of DMSO (0.1%) or JQ-1 (500 nM) were stained for a senescence-associated marker using a β-galactosidase staining kit (Beyotime; Shanghai, China).

2.12. Western blot analysis

JS-1 cells were rinsed with ice-cold PBS, harvested, and lysed in a lysis buffer (HEPES, 25 mM; 1.5% Triton X-100; 1% sodium deoxycholate; 0.1% sodium dodecyl sulfate [SDS]; NaCl, 0.5 M; EDTA, 5 mM; NaF, 50 mM; sodium vanadate, 0.1 mM;

phenylmethylsulfonyl fluoride, 1 mM; and leupeptin, 0.1 g/L; pH 7.8) containing a protease inhibitor (Roche Applied Science; Indianapolis, IN, USA). Cell lysates were solubilized in SDS sample buffer, separated by 12% SDS–polyacrylamide gel electrophoresis with 60 μg of protein loaded per lane, and transferred to a nitrocellulose membrane, which was blocked with blocking buffer (5% non-fat dry milk) for 2 h at room temperature. To detect activation of the JAK2-STAT3 signaling pathway, the membranes were then incubated with the primary antibodies against phosphorylated (p)-JAK2 (Cat. No. 3771), JAK2 (Cat. No. 3230), p-STAT3 (Cat No. 4113), STAT3 (Cat. No. 4904), and β-actin (Cat. No. 3700) (all from Cell Signaling Technology; USA), all diluted 1:1000 and incubated overnight at 4 °C. To detect the expression level of α-SMA, collagen I, and collagen III, the membranes were then incubated with the primary antibodies against α-SMA (Cat. No. 3771, Abcam; Cambridge, MA, USA), collagen Ia1 (Col1a1; Servicebio; Wuhan, China), collagen III (Col3a1; Servicebio), and GAPDH (Cat. No. 3700, Abcam) followed by incubation with the corresponding horseradish peroxidase–conjugated secondary antibody (1:3,000; EMD Millipore, MA, USA) for 2 h at room temperature. Finally, the membranes were developed by enhanced chemiluminescence solutions (Thermo Fisher Scientific) and visualized using the chemical luminescence imaging apparatus FluorChem FC3 (GeneTech; Shanghai, China). Immunoreactive bands were quantified using densitometry (multiplex band analysis from FluorChem FC3).

2.13. Statistical analysis

All data were obtained in three independent experiments, with triplicate samples used for each experiment. Data sets were analyzed with Student's *t* test using GraphPad Prism 6.01 software. Data are presented as means ± SEM. Two-sided values of $P < 0.05$

were considered statistically significant.

3. Results

3.1 JQ-1 ameliorates liver fibrosis caused by *S. japonicum*

In the seventh week after *S. japonicum* infection, mice in the experimental group were injected with JQ-1, and mice in the control group were injected with the vehicle HP-β-CD, once daily for 15 days. All mice were humanely killed after 15 days of treatment (Fig. 1A). The numbers of *S. japonicum* eggs were counted in the livers and were found to be similar in both groups (Fig. 1B). As shown in Fig. 1C, the overall color of the liver from mice in the HP-β-CD group was dark and the surface was irregular, suggestive of severe fibrosis. In comparison, the color of the liver in the JQ-1–treated group was lighter and more vivid, and the surface was relatively smooth.

Three non-continuous fixed, embedded, and sectioned liver slices were selected from nine mice for Sirius red staining and morphological analysis. As shown in Fig. 1D and 1E, Sirius red staining indicated that the area of liver fibrosis in the group treated with JQ-1 was significantly smaller than that in the control HP-β-CD group. Fibrosis was observed throughout the liver of mice in the HP-β-CD group as wide scars. By contrast, the infiltration of inflammatory cells and collagen fiber in the liver tissue was significantly reduced in the group of mice treated with JQ-1.

The degree of liver cell damage was evaluated by measuring the enzyme levels of AST and ALT in the serum of the mice. As shown in Figure 1F, serum transaminase activity in the JQ-1 group was significantly lower than that in the HP-β-CD group ($P < 0.05$). In the JQ-1 group, the level of hydroxyproline in the liver tissue of mice was also

292 significantly lower than that in the HP-β-CD group (Figure 1G, $P < 0.05$). Taken
293 together, these results indicated that the degree of liver fibrosis in the JQ-1 group was
294 significantly decreased.
295
296 **3.2 . JQ-1 treatment decreases collagen expression in the liver by reducing**
297 **activation of HSCs**
298 The immunohistochemical results showed that the expression levels of α-SMA and
299 Col1a1 in mouse liver significantly decreased after JQ-1 treatment (Fig. 2A and 2B).
300 The expression level of α-SMA was significantly lower in the JQ-1 treated group than
301 in the control group ($P < 0.05$). In addition, the expression levels of Col1a1 and Col3a1
302 in the HSCs of the JQ-1–treated group were also significantly lower than those in the
303 control group (Fig. 2C, $P < 0.05$). These results indicated that JQ-1 treatment decreased
304 the expression of collagen in the liver by inhibiting the activation of HSCs in the liver
305 to ameliorate hepatic fibrosis.
306
307 **3.3. GO and KEGG pathway enrichment analyses**
308 After RNA-sequencing analysis, we analyzed 25,228 genes (Supplemental Information
309 I). Differential gene clustering analysis results showed that compared with the HP-β-
310 CD–treated control group (Group 1; G1), there were 550 differentially expressed genes
311 (≥2-fold difference) in the JQ-1–treated group(Group 2; G2), of which 263 genes were
312 upregulated and 287 genes were downregulated ($P < 0.05$) (Figure 3A and
313 Supplemental Information II). The results of subsequent analyses using qPCR were
314 consistent with the bioinformatics analyses and identified the differentially expressed
315 genes (Fig. 3B).
316

317 The 186 downregulated genes were submitted to the Database for Annotation,
318 Visualization and Integrated Discovery (DAVID) for GO term analysis. The GO
319 annotation indicated that JQ-1 affected a broad spectrum of biological processes and
320 expression of cellular components that are known to play key roles in HSC
321 transdifferentiation into myofibroblasts. These components included the extracellular
322 regions, extracellular matrix, extracellular region part and receptor activity, regulation
323 of ion transport, lipid metabolic processes, and integrin pathway (Supplementary Table
324 2). Based on the KEGG pathway database, a pathway analysis was performed to predict
325 the significantly enriched metabolic pathways and signal transduction pathways in the
326 host differentially expressed mRNAs. The significantly enriched pathways are shown
327 in Figure 3C. There were six significant signaling pathways: xenobiotic biodegradation
328 and metabolism, lipid metabolism, cancers, metabolism of cofactor and vitamins,
329 endocrine and metabolic diseases, and carbohydrate metabolism (Supplementary Table
330 3).
331
332 **3.4. Cytology results**
333 In cytology studies, we found that although JQ-1 had no effect on cell viability (Fig.
334 4A) or senescence-associated β-galactosidase activity (Fig. 4B), it significantly
335 inhibited the proliferation of JS-1 cells (Fig. 4C). The results of a TUNEL assay (Fig.
336 4D and 4E) provided further evidence that this inhibition of JS-1 cells was specific to
337 proliferation and was not caused by apoptosis.
338
339 **3.5. JQ-1 inhibits activation of JS-1 cells**
340 We used α-SMA to assess the degree of HSC activation. Using western blot and
341 quantitative PCR analyses, we found that the expression level of α-SMA in JQ-1–

342 treated JS-1 cells was significantly lower than that in the vehicle-treated (DMSO)
343 control group (Fig. 5A; $P < 0.05$). We also found that the protein expression levels of
344 collagen as assessed with Col1a1 and Col3a1 in JQ-1–treated JS-1 cells were
345 significantly lower than those in the vehicle-treated (DMSO) control group (Fig. 5B; P
346 < 0.05). These results indicated that JQ-1 treatment decreases the expression of collagen
347 in the liver by inhibiting the activation of JS-1 cells.
348
349 **3.6. JQ-1 treatment inhibits the phosphorylation of JAK2 and STAT3 in JS-1 cells**
350 As shown in Fig. 6, the expression levels of p-JAK2 and p-STAT3 were significantly
351 decreased in JS-1 cells treated with JQ-1 compared with those in the DMSO-treated
352 (vehicle control) group ($P < 0.05$). These results suggested that JAK2 and STAT3 were
353 less active in JS-1 cells after treatment with JQ-1.
354
355 **4. Discussion**
356 Previous studies have shown that JQ-1 blocks the expression of profibrotic factors by
357 competitively binding BRD4 in the carbon tetrachloride (CCl4)-induced model of liver
358 fibrosis in mice, inhibiting the development of fibrosis [7]. However, the observed
359 effect and mechanisms in the CCl4 model may not be applicable to infectious liver
360 fibrosis. In the present study, a mouse model of liver fibrosis was generated by infection
361 with *S. japonicum* to gain insight into the effects and mechanisms underlying treatment
362 with JQ-1 in *S. japonicum* egg–induced liver fibrosis. We found that JQ-1 treatment
363 significantly attenuated *S. japonicum* egg–induced fibrosis and significantly improved
364 the gross appearance of the liver (Fig. 1). We also observed that JQ-1 treatment
365 significantly inhibited expression of α-SMA, a marker of activation of HSCs in liver
366 tissue (Fig. 1).

The process of fibrosis formation from granular tissue induced by *S. japonicum* eggs deposited in the liver is dependent on HSCs, which can undergo activation and transform into myofibroblast-like cells [9]. This activation is characterized by the gradual release of intracellular vitamin A, a high rate of cell proliferation, the synthesis of a fibrogenic matrix rich in type I or type III collagen, activation of α-SMA, and a high expression of extracellular matrix (ECM) [10]. Gradual deposition of ECM leads to structural and functional disorders of the liver [11]. Because HSCs are the main fibrogenic precursor cells in the liver, the blockade, reversal, or both of this activation determines the efficacy of antifibrotic therapy and is key for the treatment of schistosomiasis-induced liver fibrosis [12].

HSCs are typically non-proliferative in normal liver tissue but become activated after liver injury or in vitro culture [13]. Non-activated HSCs are characterized by the storage of vitamin A and the accumulation of liposomes [14]. When HSCs are stimulated and become activated, they are transdifferentiated into myofibroblasts with characteristics of hyperplasia, contraction, inflammation, the disappearance of lipid droplets, chemotaxis, and a massive deposition of ECM [13]. Our sequencing results showed that genes downregulated by JQ-1 treatment and the signaling pathways regulated by these downregulated genes were involved in vitamin metabolism, lipid metabolism, and ECM synthesis. This finding indicates that treatment with JQ-1 decreased the level of vitamin A and lipid metabolism in HSCs, resulting in a decrease in ECM content, and suggests that JQ-1 reduced the severity of liver fibrosis by inhibiting activation of HSCs. Our immunohistochemistry and western blot analysis results showed that the expression levels of collagen I and collagen III also decreased in liver tissue after

392 treatment with JQ-1.

393

394 The JAK/STAT signaling pathway transmits extracellular information from the cell
395 membrane to the nucleus to modulate the transcription of target genes, including genes
396 whose protein products are crucial for defense against pathogens, differentiation,
397 proliferation, and apoptosis [15]. The JAK2/STAT3 signaling pathway is directly
398 involved in HSC activation and transdifferentiation and subsequent formation of
399 hepatic fibrosis [16]. The blockade of the JAK2/STAT3 signaling pathway impedes the
400 morphological transdifferentiation of HSCs and reduces mRNA expression of
401 profibrotic genes [17]. Cao et al. (2019) found that intragastric administration of
402 dextran sulfate sodium reduced hepatic fibrosis by inhibiting the JAK2/STAT3
403 signaling pathway, both in vitro and in vivo [18]. Magnesium isoglycyrrhizinate
404 ameliorates high fructose-induced liver fibrosis in rats via inhibiting the JAK2/STAT3
405 signaling pathway and TGF-β1/Smad signaling [19].

406

407 Recent studies have shown that JQ-1 inhibits the growth of pancreatic cancer cells,
408 regulates the expression of inflammatory cytokines associated with tumor growth, and
409 regulates the expression of several proteins known to be important in pancreatic cancer,
410 such as c-Myc, p-Erk1/2, interleukin 6, and p-STAT3 [20]. Moreover, a study
411 investigating JQ-1 treatment of acute myeloid leukemia cells indicated that this
412 treatment inhibits the expression of p-STAT3 [21]. JQ-1 has been shown to inhibit
413 CCl4-induced liver fibrosis by preventing HSC activation; however, the mechanism
414 underlying the inhibition of HSC activation requires further study [7, 22].

415

To further investigate the mechanism by which JQ-1 inhibits HSC activation in the present study, the mouse HSC line (JS-1 cells) was cultured and JQ-1 administered in subsequent in vitro experiments. We found that the expression levels of p-JAK2 and p-STAT3 were significantly reduced in the JQ-1 treated JS-1 cells (Fig. 6), suggesting that JQ-1 inhibits activation of HSCs by suppressing the phosphorylation of JAK2 and STAT3. As shown in Fig. 7, JQ-1 inhibits the JAK2/STAT3 signaling pathway in JS-1 cells, thereby blocking the activation and proliferation of HSCs and reducing the severity of liver fibrosis. JQ-1 can inhibit all BET proteins that disturb the binding of BET to acetylated lysine, which can regulate numerous targets to affect hepatic fibrosis. Suppressing JAK2 and STAT3 activation may be a JQ-1 mechanism that inhibits schistosomal hepatic fibrosis. However, our study did not determine whether one of the BET proteins is responsible for the transcription of genes involved in the activation and proliferation of HSCs; thus, the underlying mechanism requires future investigation.

In summary, the administration of JQ-1 decreased the degree of liver fibrosis caused by *S. japonicum*. JQ-1 inhibited the activation and proliferation of HSCs by blocking the phosphorylation of JAK2 and STAT3 in the JAK2/STAT3 signaling pathway to achieve this therapeutic effect. Our study provides new insight into the potential development of new therapeutic strategies for *Schistosoma*-induced liver fibrosis.

Acknowledgments

We thank a native English speaker (Science/Medical English Editing for International Researchers) for modifying the manuscript.

Funding Statement

This work was supported by grants from the National Natural Science Foundation of

China (http://www.nsfc.gov.cn) (grant numbers 81471982) and Key University Science Research Project of Anhui Province of China (KJ2019A0223). The funders had no role in study design, data collection and analysis, decision to publish, or preparation of the manuscript.

Data Availability

All relevant data are within the manuscript and its Supporting Information files.

References

1. McManus DP, Gray DJ, Li Y, Feng Z, Williams GM, Stewart D, Rey-Ladino J, Ross AG. Schistosomiasis in the People's Republic of China: the era of the Three Gorges Dam. Clin Microbiol Rev. 2010;23(2):442-66. doi: 10.1128/CMR.00044-09.
2. Wu W, Feng A, Huang Y. Research and control of advanced schistosomiasis japonica in China. Parasitol Res. 2015;114(1):17-27. doi: 10.1007/s00436-014-4225-x.
3. Sathiyamoorthy G, Sehgal S, Ashton RW. Pirfenidone and Nintedanib for Treatment of Idiopathic Pulmonary Fibrosis. South Med J. 2017;110(6):393-398. doi: 10.14423/SMJ.0000000000000655.
4. Belkina AC, Denis GV. BET domain co-regulators in obesity, inflammation and cancer. Nat Rev Cancer. 2012;12(7):465-77. doi: 10.1038/nrc3256.
5. Dawson MA, Kouzarides T. Cancer epigenetics: from mechanism to therapy. Cell. 2012;150(1):12-27. doi: 10.1016/j.cell.2012.06.013.
6. Ferri E, Petosa C, McKenna CE. Bromodomains: Structure, function and pharmacology of inhibition. Biochem Pharmacol. 2016;106:1-18. doi: 10.1016/j.bcp.2015.12.005. Epub 2015 Dec 18. PMID: 26707800.
7. Ding N, Hah N, Yu RT, Sherman MH, Benner C, Leblanc M, He M, Liddle C, Downes M, Evans RM. BRD4 is a novel therapeutic target for liver fibrosis. Proc Natl Acad Sci U S A. 2015 ;112(51):15713-8. doi: 10.1073/pnas.1522163112.
8. Tang X, Peng R, Phillips JE, Deguzman J, Ren Y, Apparsundaram S, Luo Q, Bauer

CM, Fuentes ME, DeMartino JA, Tyagi G, Garrido R, Hogaboam CM, Denton CP, Holmes AM, Kitson C, Stevenson CS, Budd DC. Assessment of Brd4 inhibition in idiopathic pulmonary fibrosis lung fibroblasts and in vivo models of lung fibrosis. Am J Pathol. 2013;183(2):470-9. doi: 10.1016/j.ajpath.2013.04.020.

9. Carson JP, Ramm GA, Robinson MW, McManus DP, Gobert GN. Schistosome-Induced Fibrotic Disease: The Role of Hepatic Stellate Cells. Trends Parasitol. 2018;34(6):524-540. doi: 10.1016/j.pt.2018.02.005.
10. Reeves HL, Friedman SL. Activation of hepatic stellate cells--a key issue in liver fibrosis. Front Biosci. 2002;7:d808-26. doi: 10.2741/reeves.
11. Neubauer K, Saile B, Ramadori G. Liver fibrosis and altered matrix synthesis. Can J Gastroenterol. 2001;15(3):187–193. doi:10.1155/2001/870205.
12. Li H, Hua J, Guo CX, Wang WX, Wang BJ, Yang DL, Wei P, Lu YP. Pentoxifylline inhibits liver fibrosis via hedgehog signaling pathway. J Huazhong Univ Sci Technolog Med Sci. 2016;36(3):372-376. doi: 10.1007/s11596-016-1594-7.
13. Puche et al., 2013 Puche JE, Saiman Y, Friedman SL. Hepatic stellate cells and liver fibrosis. Compr Physiol. 2013;3(4):1473-92. doi: 10.1002/cphy.c120035.
14. Molenaar MR, Vaandrager AB, Helms JB. Some Lipid Droplets Are More Equal Than Others: Different Metabolic Lipid Droplet Pools in Hepatic Stellate Cells. Lipid Insights. 2017;10:1178635317747281. doi: 10.1177/1178635317747281.
15. Morris R, Kershaw NJ, Babon JJ. The molecular details of cytokine signaling via the JAK/STAT pathway. Protein Sci. 2018;27(12):1984-2009. doi: 10.1002/pro.3519.
16. Cao et al., 2007 Cao Q, Mak KM, Lieber CS. Leptin represses matrix metalloproteinase-1 gene expression in LX2 human hepatic stellate cells. J Hepatol. 2007;46(1):124-33. doi: 10.1016/j.jhep.2006.07.027.
17. Lakner AM, Moore CC, Gulledge AA, Schrum LW. Daily genetic profiling indicates JAK/STAT signaling promotes early hepatic stellate cell transdifferentiation. World J Gastroenterol. 2010;16(40):5047-56. doi: 10.3748/wjg.v16.i40.5047.
18. Cao G, Zhu R, Jiang T, Tang D, Kwan HY, Su T. Danshensu, a novel indoleamine

2,3-dioxygenase1 inhibitor, exerts anti-hepatic fibrosis effects via inhibition of JAK2-STAT3 signaling. Phytomedicine. 2019;63:153055. doi: 10.1016/j.phymed.2019.153055.

19. Yang YZ, Zhao XJ, Xu HJ, Wang SC, Pan Y, Wang SJ, Xu Q, Jiao RQ, Gu HM, Kong LD. Magnesium isoglycyrrhizinate ameliorates high fructose-induced liver fibrosis in rat by increasing miR-375-3p to suppress JAK2/STAT3 pathway and TGF-β1/Smad signaling. Acta Pharmacol Sin. 2019;40(7):879-894. doi: 10.1038/s41401-018-0194-4.
20. Leal AS, Williams CR, Royce DB, Pioli PA, Sporn MB, Liby KT. Bromodomain inhibitors, JQ1 and I-BET 762, as potential therapies for pancreatic cancer. Cancer Lett. 2017;394:76-87. doi: 10.1016/j.canlet.2017.02.021.
21. Belkina AC, Nikolajczyk BS, Denis GV. BET protein function is required for inflammation: Brd2 genetic disruption and BET inhibitor JQ1 impair mouse macrophage inflammatory responses. J Immunol. 2013;190(7):3670-8. doi: 10.4049/jimmunol.1202838.
22. Hassan R, Tammam SN, Safy SE, Abdel-Halim M, Asimakopoulou A, Weiskirchen R, Mansour S. Prevention of hepatic stellate cell activation using JQ1- and atorvastatin-loaded chitosan nanoparticles as a promising approach in therapy of liver fibrosis. Eur J Pharm Biopharm. 2019;134:96-106. doi: 10.1016/j.ejpb.2018.11.018.

Figure legend

Fig. 1. JQ-1 treatment ameliorates liver fibrosis caused by *S. japonicum*.

(A) Therapeutic regimen used in the mouse model of liver fibrosis. (B) Effect of JQ-1 or vehicle (HP-β-CD) treatment on the number of eggs per gram in the liver. (C) Effect of JQ-1 treatment on general liver morphology of mice infected with *S. japonicum*. (D) Effect of JQ-1 treatment on hepatic fibrosis in mice infected with *S. japonicum*. (E) Area of the liver with hepatic fibrosis as measured by computer-assisted morphometric analysis. (F) Effect of JQ-1 treatment on serum alanine aminotransferase

(ALT) and aspartate aminotransferase (AST) levels and (G) liver hydroxyproline levels in mice infected with *S. japonicum*. Data represent the mean ± SEM (n = 9 for each group). Asterisks denote statistically significant differences (Student's *t* test, $P < 0.05$) vs. the HP-β-CD–treated control group.

Fig. 2 Effect of JQ-1 treatment on expression levels of α-SMA and collagen in mouse liver. Immunohistochemistry images of (A) α-SMA and (B) Col1a1 expression in mouse liver after JQ-1 or vehicle (HP-β-CD) treatment. (C) Quantitative PCR analysis of liver α-SMA and liver collagen protein levels after JQ-1 or vehicle (HP-β-CD) treatment in mice. Data represent the mean ± SEM (n = 9 for each group). each performed in triplicate. Asterisks denote statistically significant differences (Student's *t* test, $*P < 0.05$).

Fig. 3 Bioinformatics Analysis. (A) Heat map of differential clustering analysis of mRNA in the JQ-1 treated group (Group 2; G2) versus the HP-β-CD group (Group 1; G1). (B) Differentially expressed genes identified using quantitative PCR. The mRNA levels are expressed relative to those in controls following normalization to GAPDH. Data represent the mean ± SEM (n = 9 for each group). Asterisks denote statistically significant differences (Student's *t* test, $*P < 0.05$) vs. HP-β-CD group. (C) KEGG analysis of downregulated genes involved in the metabolic pathway of the proteins. The abscissa indicates *P* values; red bars, highly enriched and meaningful metabolic pathways; and blue bars, a less enriched and reference metabolic pathway. The ordinate shows the name of the metabolic pathway.

Fig. 4 Effect of JQ-1 treatment on hepatic stellate cell (HSC) activity, aging,

554 **proliferation, and apoptosis.**

555 (A) Cell viability of JQ-1–treated (500 nM) HSCs as measured by trypan blue staining.
556 (B) Cellular senescence of JQ-1–treated (500 nM) HSCs measured by β-galactosidase
557 staining. (C) Cell proliferation of JQ-1–treated (500 nM) HSCs measured by CCK-8
558 (*$P < 0.05$). OD represents optical density. (D) Apoptosis in JQ-1–treated (500 nM)
559 HSCs measured by a TUNEL assay. Data represent the mean ± SEM of at least three
560 independent experiments, each performed in triplicate. Asterisks denote statistically
561 significant differences (Student's *t* test, *$P < 0.05$).

562

563 **Fig. 5 Effect of JQ-1 treatment on the expression levels of α-SMA and collagen in**
564 **hepatic stellate cells (HSCs).** (A) Representative western blot images for α-SMA,
565 Col1a1, and Col3a1 in HSCs after JQ-1 treatment.(B) Relative quantitative PCR
566 analysis of α-SMA and collagen levels in HSCs after JQ-1 treatment. Data represent
567 the mean ± SEM of at least three independent experiments, each performed in triplicate.
568 Asterisks denote statistically significant differences (Student's *t* test, *$P < 0.05$).

569

570 **Fig. 6 JQ-1 inhibits STAT3 and JAK2 phosphorylation.** (A) Representative western
571 blot images for JAK2, phosphorylated (p)-JAK2, STAT3, and p-STAT3 in JS-1 cells
572 after JQ-1 or vehicle control (DMSO) treatment.(B) Relative quantitative analysis of
573 JAK2, p-JAK2, STAT3, and p-STAT3 levels. β-Actin was used as an internal control.
574 Data represent the mean ± SEM of at least three independent experiments, each
575 performed in triplicate. Asterisks denote statistically significant differences (Student's
576 *t* test, *$P < 0.05$).

577

578 **Fig. 7 Schematic diagram of the inhibition of hepatic stellate cell (HSC) activation**

and proliferation by JQ-1.

JQ-1 blocks downstream transcriptional regulation by binding to BRD4, thereby blocking phosphorylation of JAK2 and STAT3 in the JAK2/STAT3 signaling pathway and inhibiting HSC activation and proliferation.

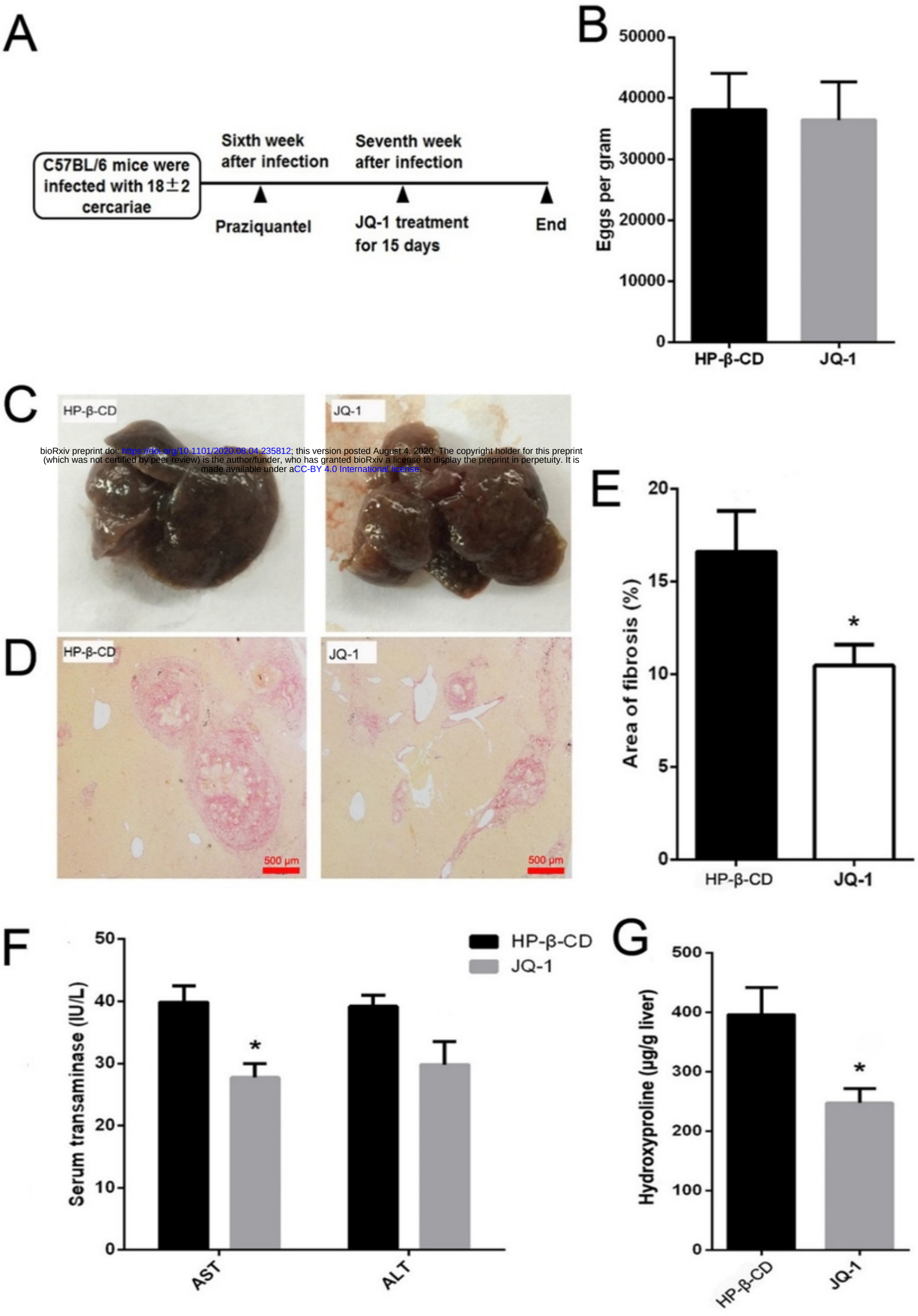

Fig 1

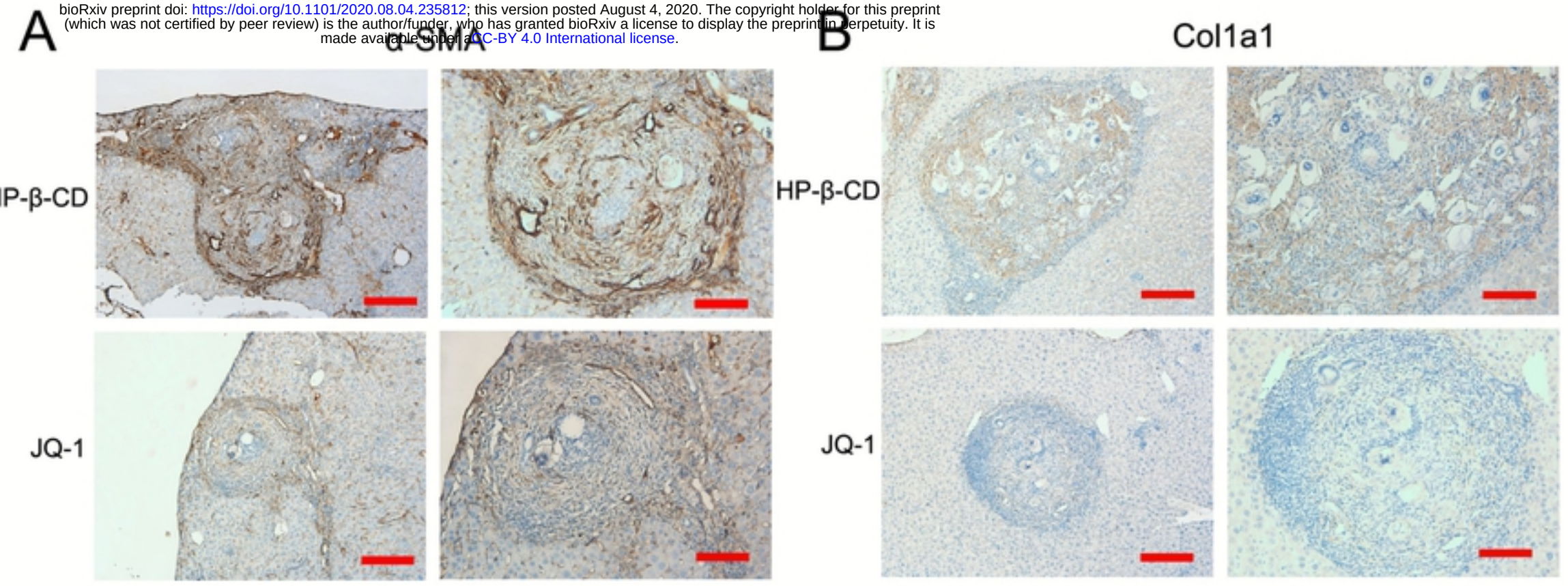

Fig 2

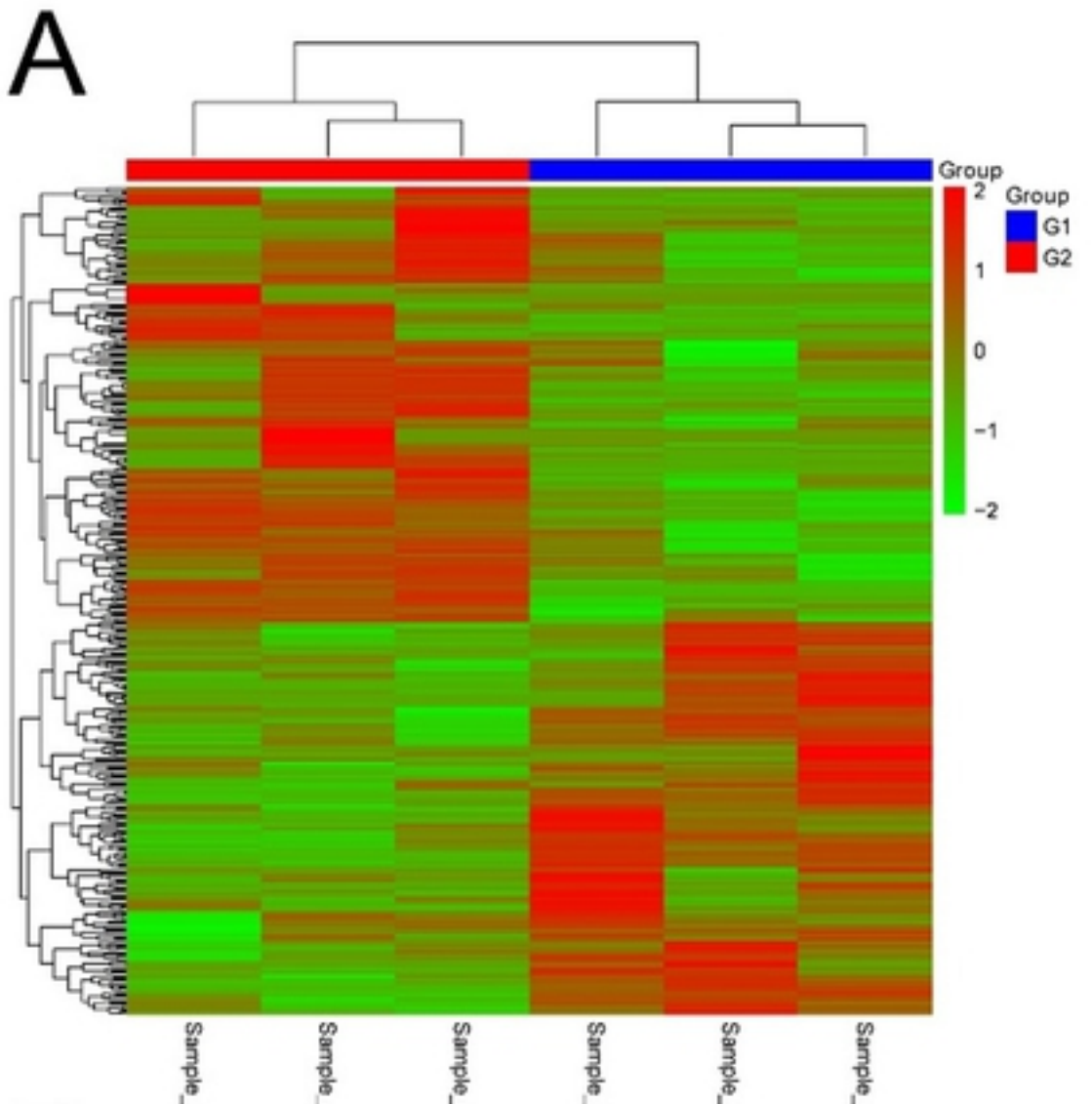

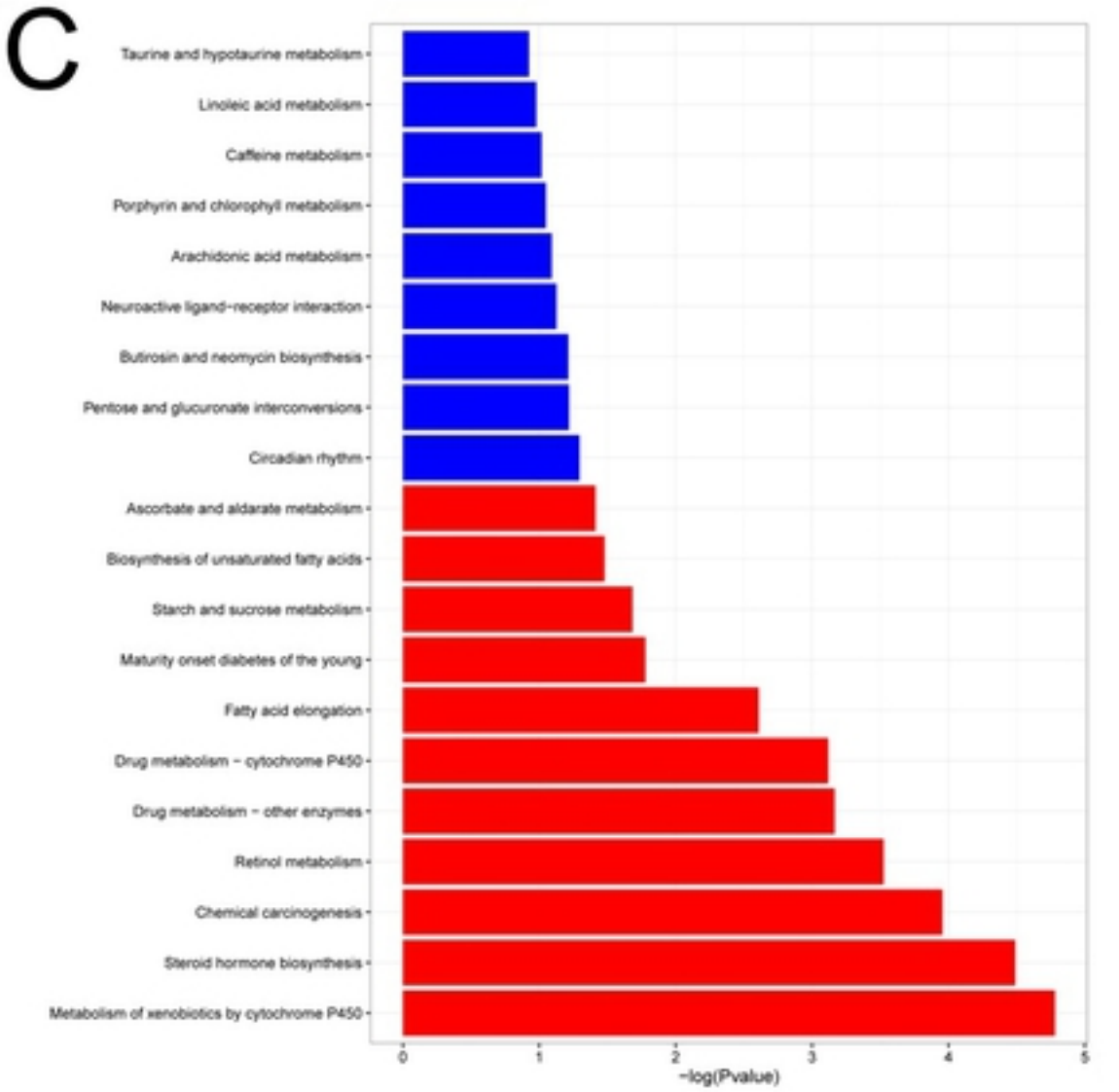

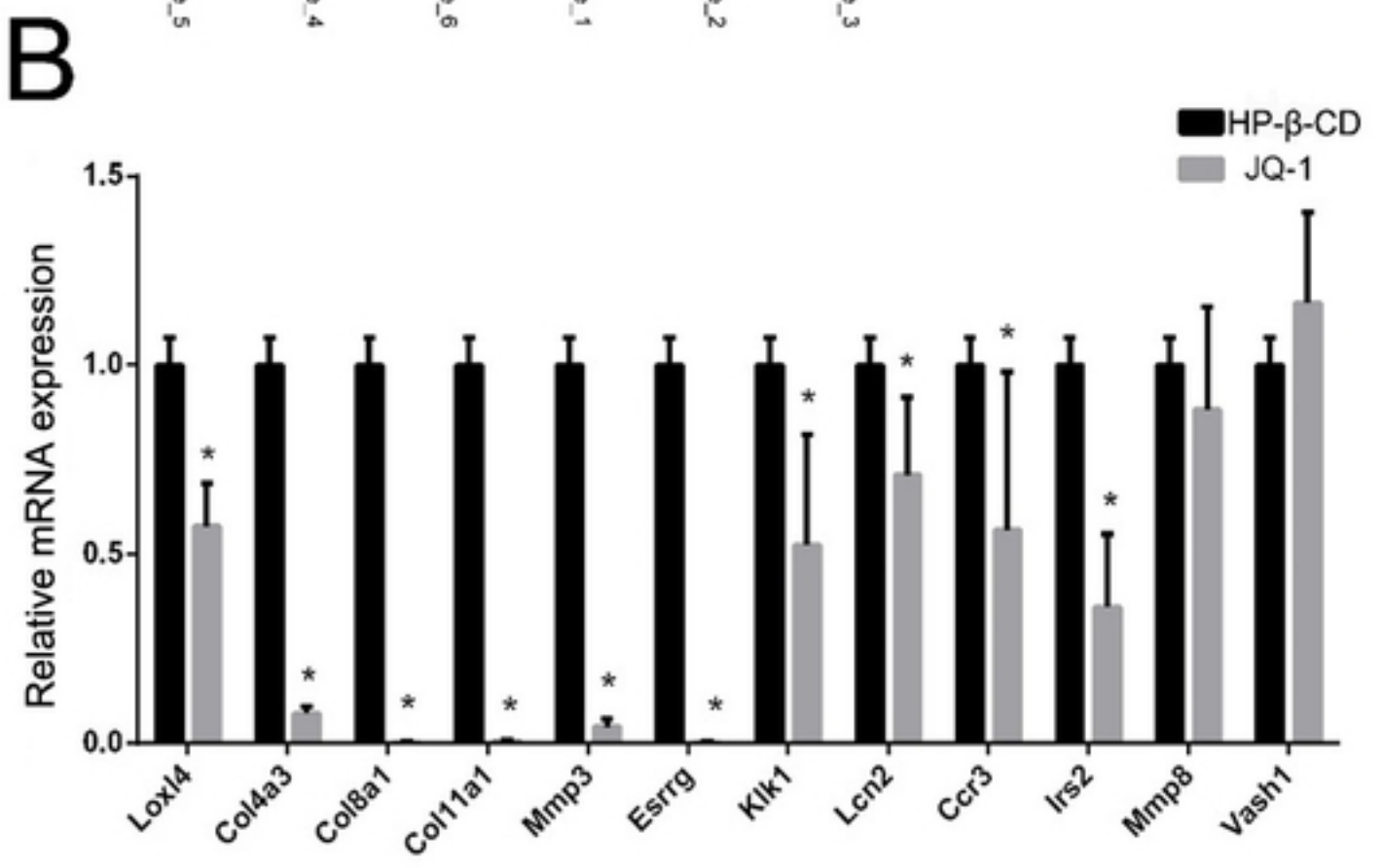

Fig 3

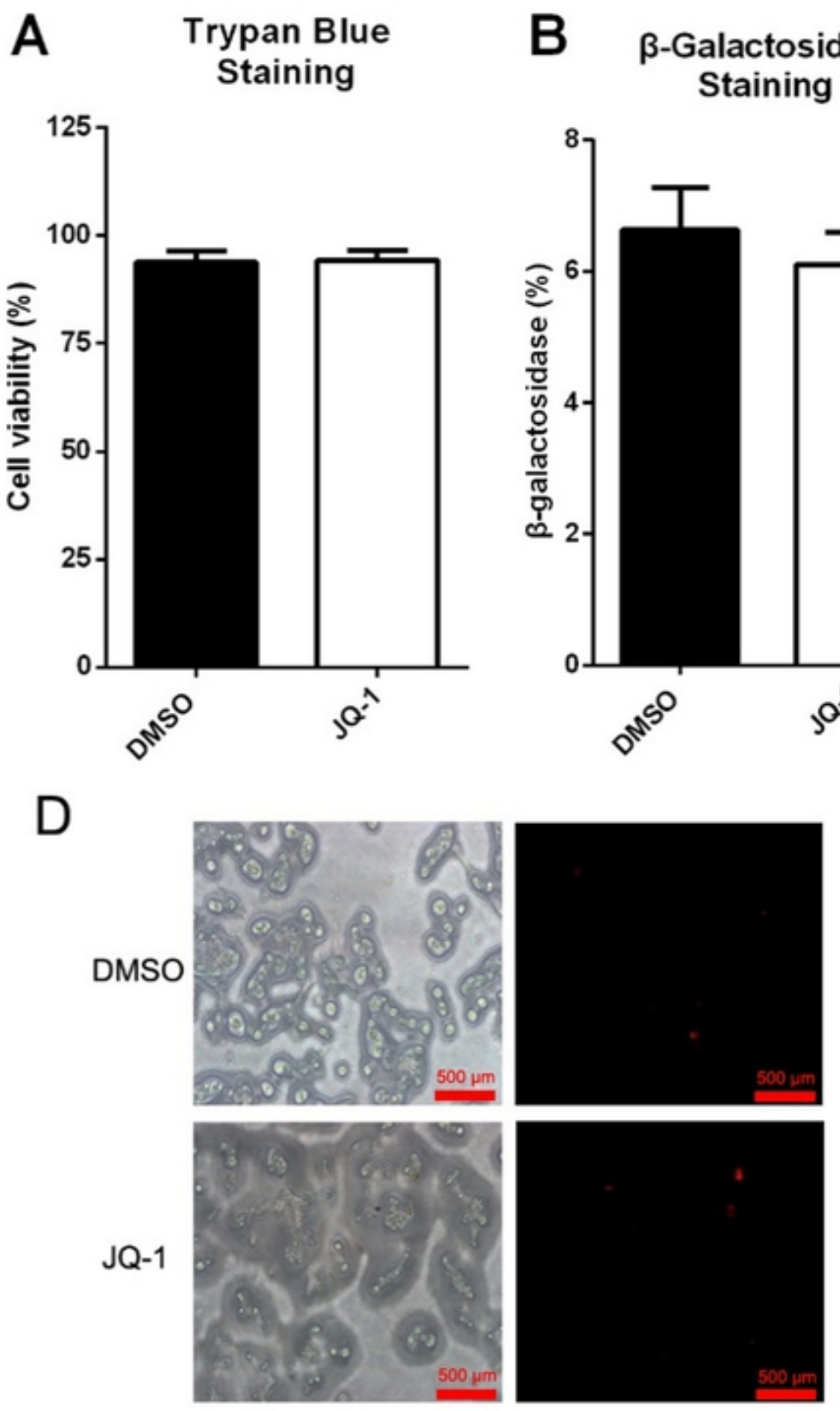
A
Trypan Blue Staining
Cell viability (%)
125
100
75
50
25
0
DMSO
JQ-1
B
β-Galactosidase Staining
β-galactosidase (%)
8
6
4
2
0
DMSO
JQ-1
C
JQ-1
DMSO
CCK-8 assay OD (450 nm)
1.5
1.0
0.5
0.0
*
0 h
12 h
24 h
D
DMSO
JQ-1
500 μm
E
TUNEL Staining
TUNEL (%)
10
8
6
4
2
0
DMSO
JQ-1

Fig 4

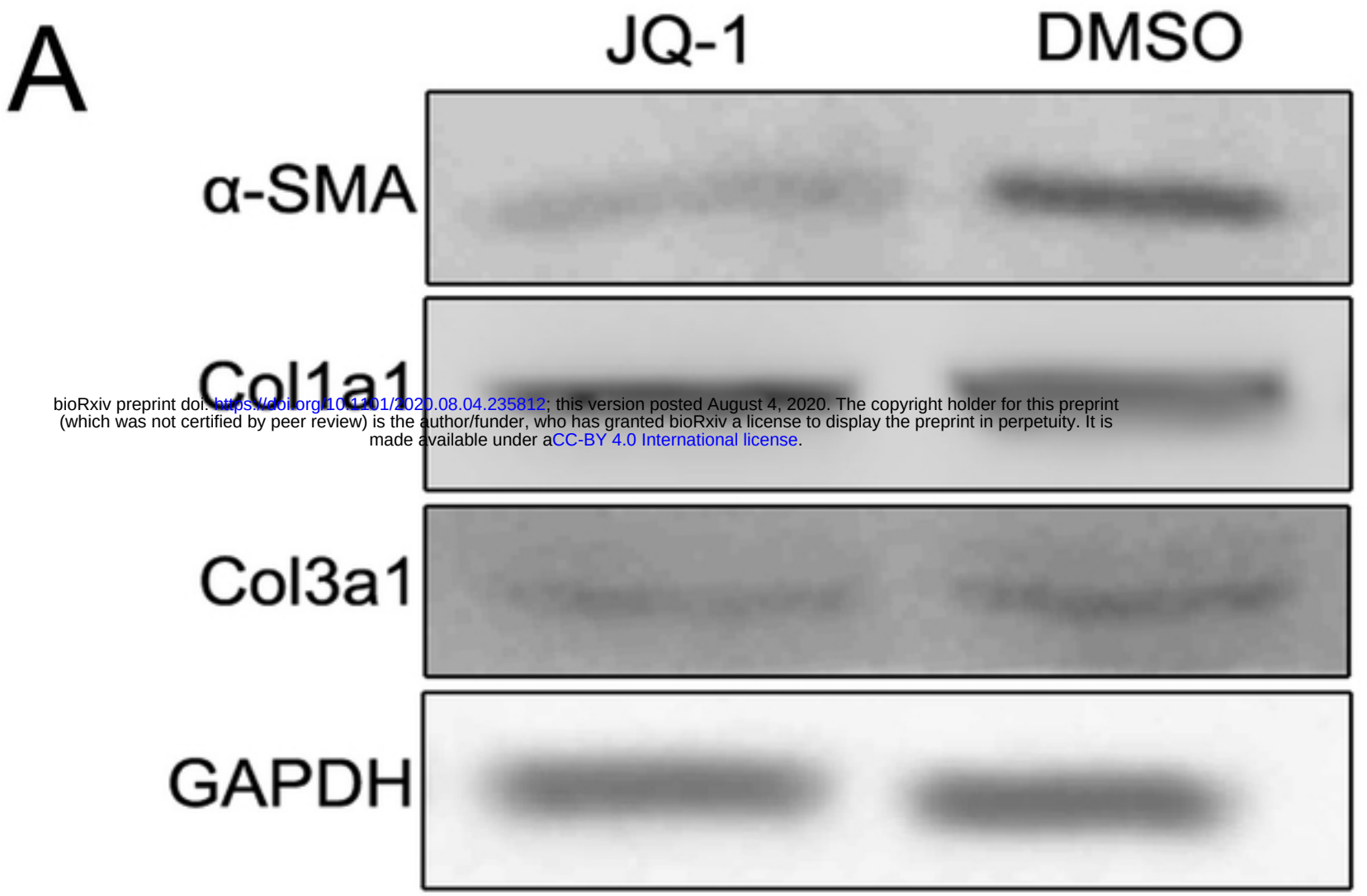

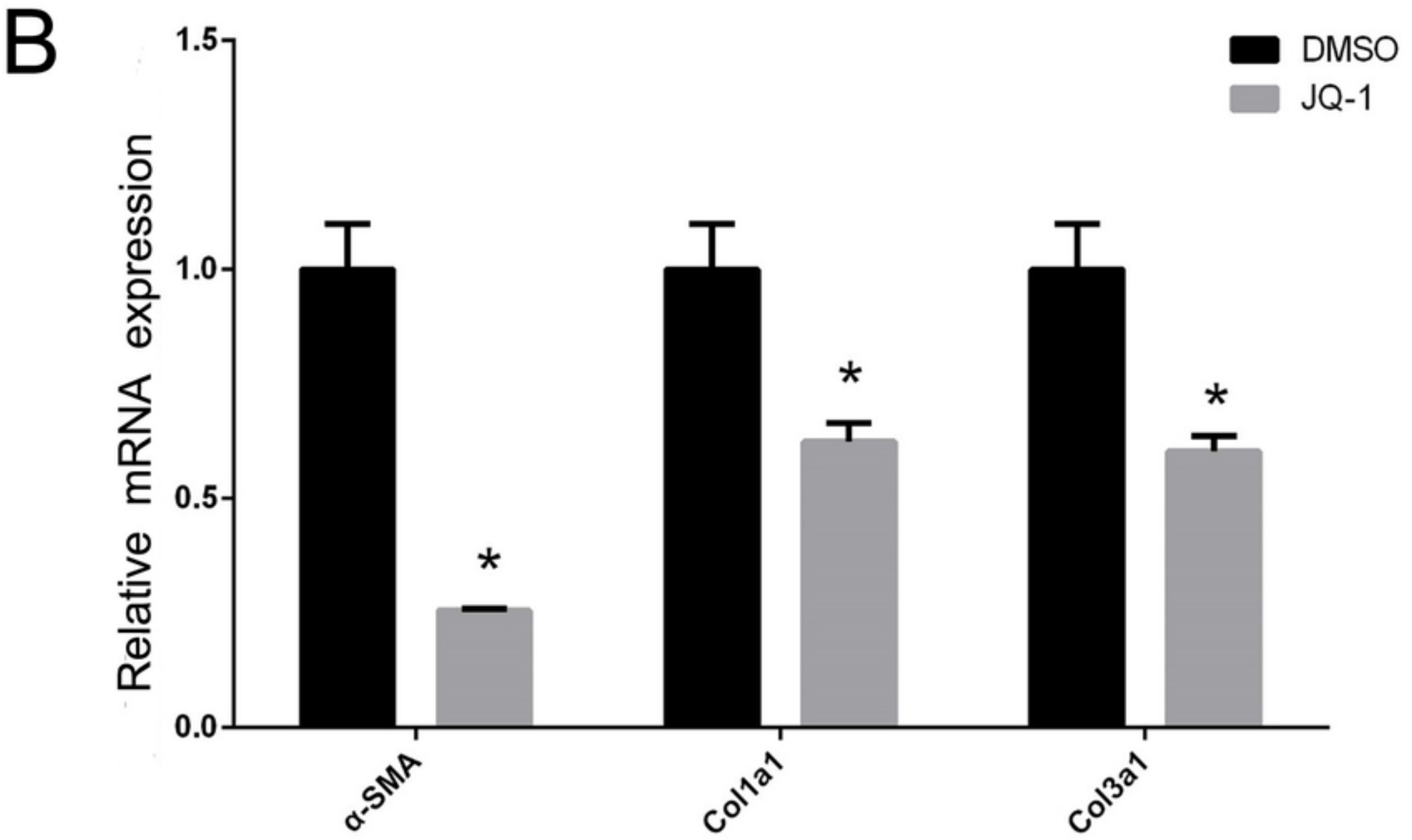

Fig 5

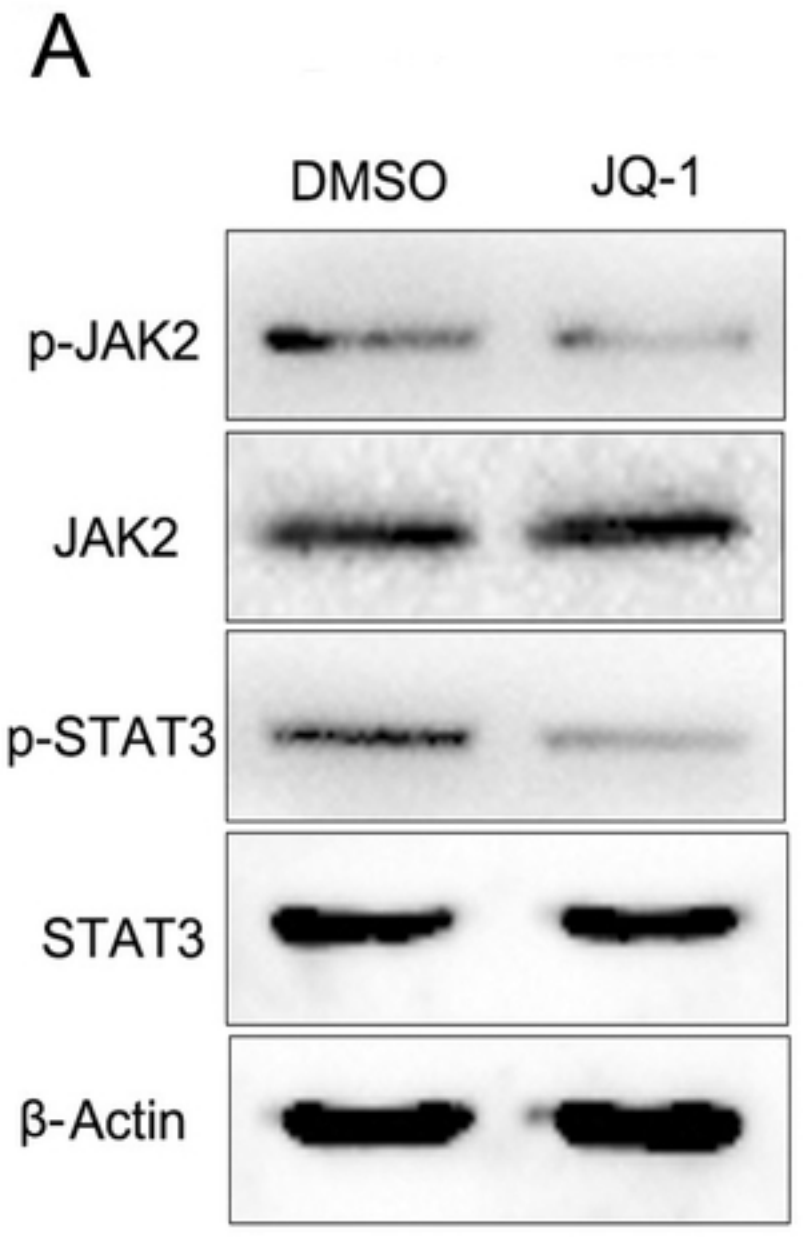
A
DMSO
JQ-1
p-JAK2
JAK2
p-STAT3
STAT3
β-Actin

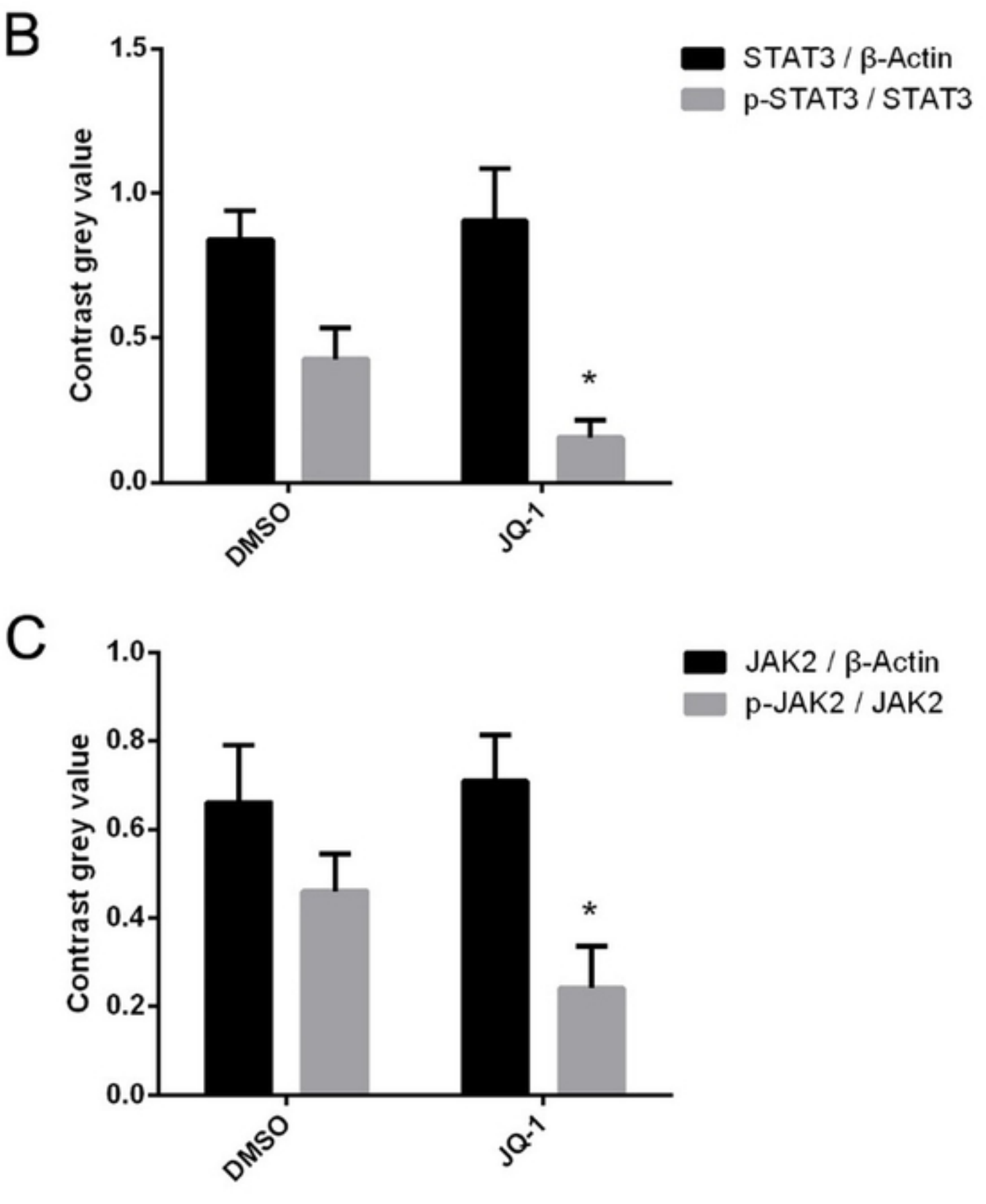
B
STAT3 / β-Actin
p-STAT3 / STAT3
Contrast grey value
1.5
1.0
0.5
0.0
*
DMSO
JQ-1
C
JAK2 / β-Actin
p-JAK2 / JAK2
Contrast grey value
1.0
0.8
0.6
0.4
0.2
0.0
*
DMSO
JQ-1

Fig 6

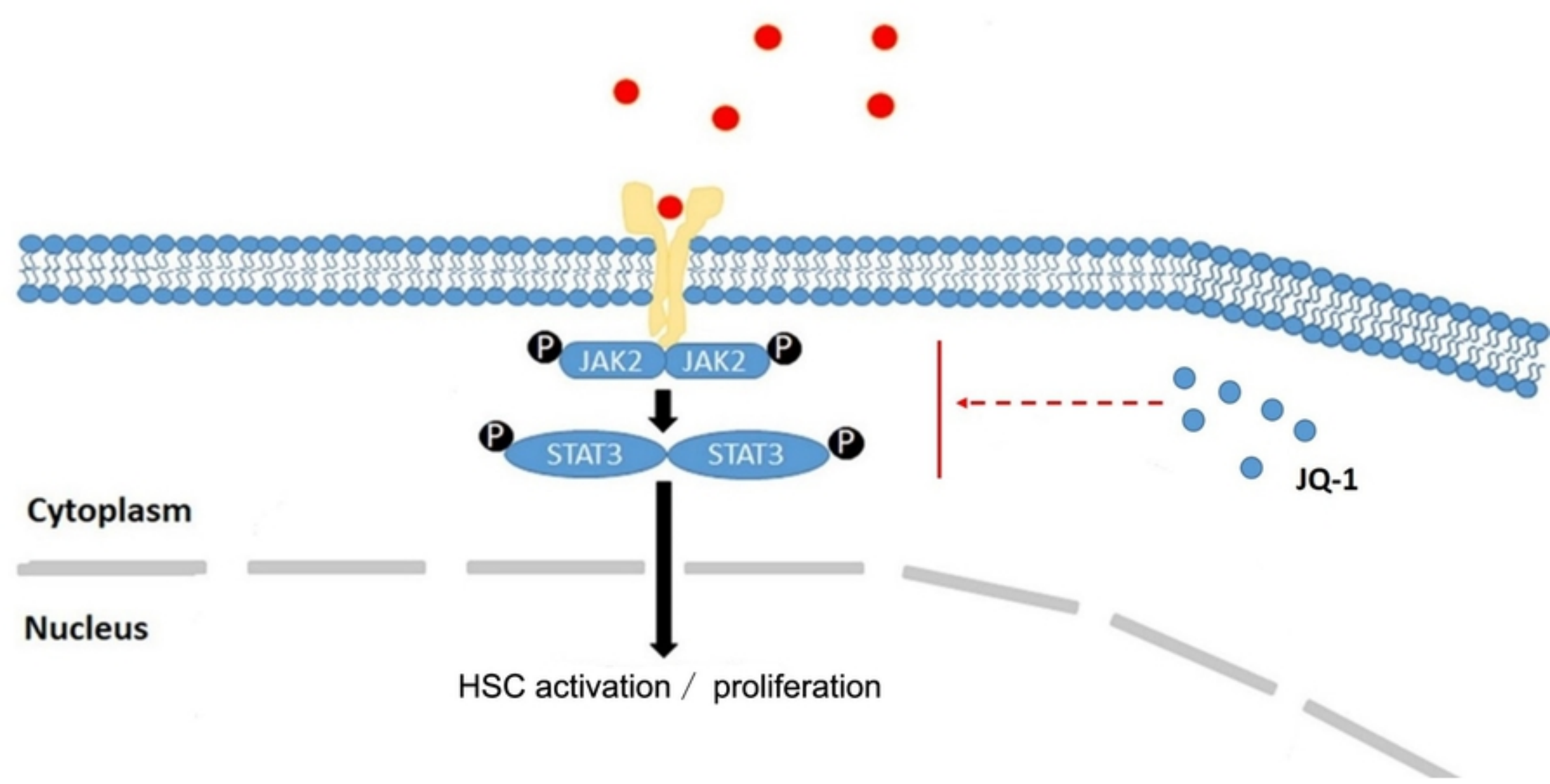
P
JAK2
JAK2
P
P
STAT3
STAT3
P
JQ-1
Cytoplasm
Nucleus
HSC activation / proliferation

Fig 7